振动焊接技术在大型焊接构件中的应用

卢庆华， 陈立功， 倪纯珍， 饶德林
（上海交通大学 材料科学与工程学院，上海 200030）

卢庆华

摘 要：在高炉用钢厚板电渣焊中应用振动调制工艺。接头金相组织显示，附加振动后，焊接接头晶粒细化明显。研究三种振动加速度（0，3，6 m/s^2）下焊接接头的残余应力和侧弯性能。焊接变形是 H 型钢焊接时存在的主要问题。采用埋弧振动焊接可明显减小 H 型钢的焊接变形。结果表明，合理的振动调制工艺可以有效地减小残余应力并改善焊接接头的综合性能，控制变形，保证生产质量。

关键词：振动焊接；侧弯；H 型钢；焊接变形
中图分类号：TG448 文献标识码：A 文章编号：0253－360X(2007)02－092－04

0 序 言

大型焊接结构制造的共同问题[1,2]是，大热输入焊接造成晶粒粗大，以及焊接变形和残余应力的必然存在将明显影响产品的质量，传统的方法是热时效工艺；但在实际工程中，当结构过大导致工艺投资与能耗过大，或由于结构复杂使热时效工艺难以实施，或由于异种材料构造对工艺温度有限制时，传统的热时效工艺将受到限制。

振动焊接（vibratory weld conditioning，VWC）是一种优化焊接结构品质的新工艺[3,4]，它是在焊接过程中施加机械振动外场，利用焊接热场及应用振动动应力在金属凝固－结晶过程细化晶粒和减小凝固过程应力，使焊接接头的质量明显优化[5－7]。

试验中，将振动焊接技术分别应用于高炉厚板立缝电渣焊及 H 型钢埋弧焊[8]中，研究机械振动对接头性能的影响，探索不同振动加速度下接头性能变化规律，并研究振动焊接对焊接变形的影响。

1 振动焊接在高炉用钢厚板电渣焊中的应用

1.1 试验材料及方法

试验用板材为 BB503，长度 1 000 mm，宽度 500 mm，厚度 90 mm；焊丝为 H08MnMoA，ϕ3.0 mm。两块平板通过电渣焊连接。将工件分为上、下两部分，分别采用不同的振幅予以振动。从工件底部至工件长度的一半位置，控制振动加速度为 3 m/s^2；从工件长度的一半位置至工件顶端，控制振动加速度为 6 m/s^2。

1.2 试验结果

1.2.1 金相分析

对振动加速度分别为 0，3，6 m/s^2 三种工况的焊接接头的金相组织进行分析。图 1 示出了三种振动加速度下焊缝的金相组织。显然，随振动幅度的加大，接头金属的细化程度也加大，且作用明显。

1.2.2 焊接残余应力

焊接完毕待冷却后，运用盲孔法测试焊接残余应力，结果如表 1 所示。由表 1 可见，总体残余应力水平不高，且 3 m/s^2 加速度下的焊接残余应力值明显低于 6 m/s^2 的工况，这是因为 3 m/s^2 加速度时经历的振动时间较 6 m/s^2 的长。焊后最大残余应力随着振动输入能量的增大而减小，这说明振动调制焊接完后继续振动一段时间，以增加振动输入的能量，对减小残余应力有利。

表 1 振动焊接残余应力测试结果

Table 1 Results of residual stress in VWC

振动加速度度 a/(m·s^{-2})	最大主残余应力 R_{rmax}/MPa	最小主残余应力 R_{min}/MPa	剪应力 τ/MPa	纵向残余应力 R_{rx}/MPa	横向残余应力 R_{ry}/MPa
3	168	109	59	160	118
6	236	152	84	231	157

收稿日期：2006－03－06

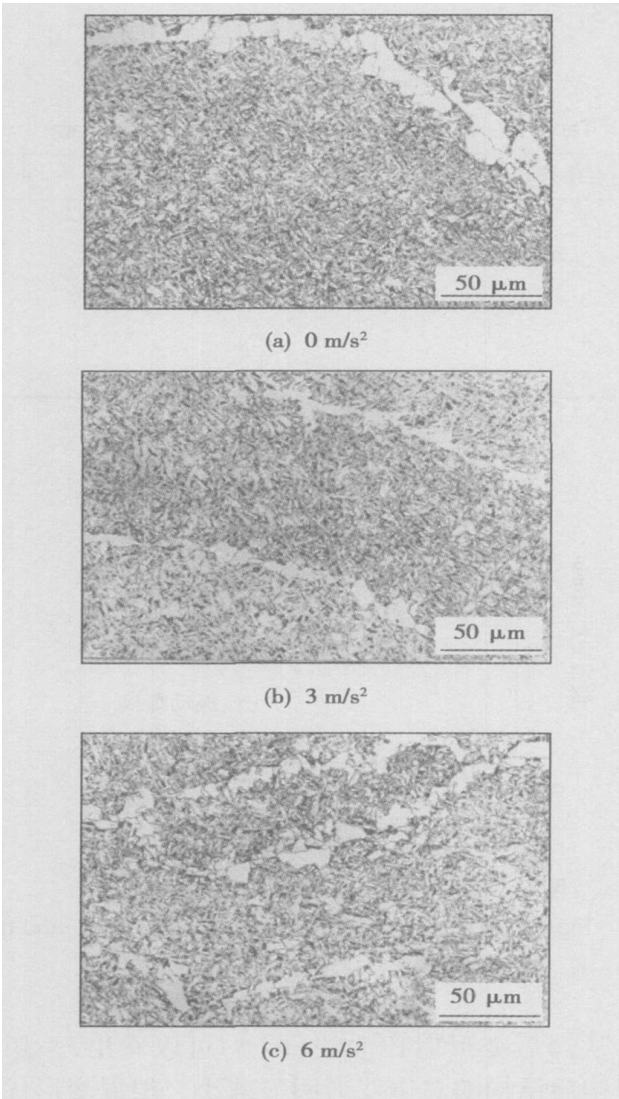

图 1　不同振动加速度下的焊缝组织

Fig. 1　Weld microstructure in different vibratory acceleration conditions

1.2.3　180° 侧弯试验

侧弯性能是高炉钢电渣焊焊缝的重要指标之一, 提高侧弯合格率是采用附加振动工艺的重要原因。对振动加速度为 0, 3, 6 m/s² 三种工况下的焊接接头进行 180° 侧弯试验, 试样受拉面为焊缝纵剖面, 试样取样及尺寸按国家标准GB 2653－1989 进行, 试验结果如表 2 所示, 可见振动焊接工艺可以改善侧弯性能。其中, 在振动加速度为 6 m/s² 时, 侧弯合格率为 100%。

表 2　三种工况的侧弯试验结果

(开裂数/试样总数)

Table 2　Results of side bend test in different vibratory acceleration conditions(cracked number/total number)

	振动加速度 a/(m·s^{-2})		
	0	3	6
180° 侧弯	3/8	2/8	0/8
合格率 η(%)	58.3	75	100

2　振动焊接在 H 型钢埋弧焊中的应用

各种 H 型钢因其强度高、质量轻、耐用性好及易于改造等优点在框架结构中被越来越广泛采用。H 型钢焊接后, 容易发生焊接变形, 主要有纵向收缩变形、翼板的角变形、弯曲变形、波浪变形和扭曲变形[9]。

2.1　振动焊接工艺

2.1.1　焊前准备

H 型钢规格为 H900 mm×200 mm ×6/8 mm, 长 6 m, 材质为 Q235B。先在平台上进行组立。组立好的工件安放在工装上, 用焊条电弧焊点焊定位, 通过 4 个托架实现对工件的稳定支承, 用斜契块把底部翼板垫平。

2.1.2　H 型钢的振动焊接工艺

采用船形振动埋弧自动焊[10], 装配顺序如图 2 所示。电弧电压 32～33 V, 焊接电流 500 A, 焊接速度 0.60 m/min; 焊丝为 φ4 mm 的 H08A, 焊剂 HJ431。激振器固定在工件顶部翼板中央, 偏心旋转面与腹板平行。每焊一道焊缝, 工件翻身一次, 并更换一次激振器的位置, 但激振器与当前焊缝始终保持如图 3 所示的相对位置。焊接前, 两端头均要增加引弧板, 焊接时用斜契块把底部翼板压紧。

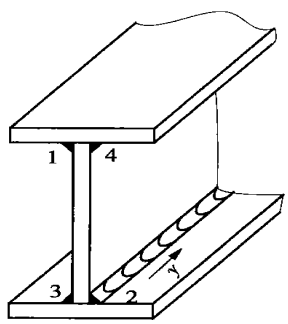

图 2　焊接顺序

Fig. 2　Welding sequence

2.1.3　非振动焊接工艺

H 型钢规格、焊接方法、焊接材料及焊接电流、焊接速度、电弧电压等焊接工艺同 H 型钢振动焊接工艺, 但不施加振动。

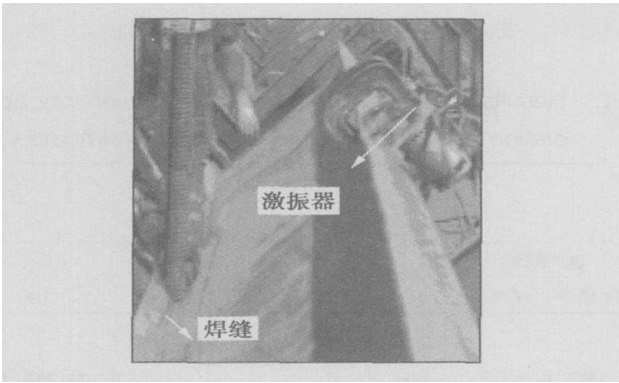

图 3 激振器与焊缝的相对位置

Fig. 3 Relative position of vibration exciter and weld

2.2 试验工艺数据与结果分析

通过测量 6 m 长腹板各处的波浪变形，得到了腹板上波浪变形最大的 4 个值，如图 4 所示。

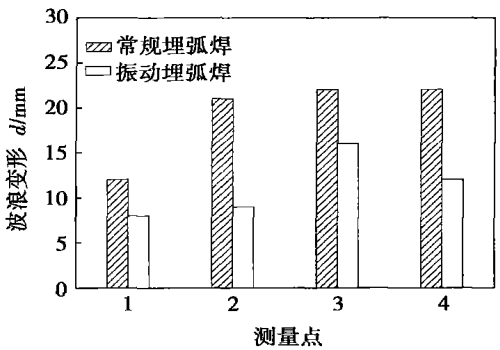

图 4 两种埋弧焊工艺下的波浪变形比较

Fig. 4 Comparison of wave transformation in two kinds of SAW

从测量结果看，采用振动埋弧焊接工艺，测量得 H 型钢腹板波浪变形的最大值为 16 mm，波浪变形最大 4 个点的平均值是 11.3 mm；不采用附加振动的常规埋弧焊接工艺，腹板波浪变形的最大值为 22 mm，波浪变形最大 4 个点的平均值是 19.3 mm，显然，振动焊接工艺下，焊后波浪变形减小。

焊接变形的产生与焊接过程不均匀加热有关，机械振动加剧了焊缝熔池金属的运动，加速了焊接过程的热传导，使焊缝及热影响区金属的温度分布比不加振动时更均匀，接头金属的不均匀塑性变形减小，导致焊接残余应力和焊接变形减小；另外，振动焊接工艺由于对接头晶粒的细化，也减小了金属凝固过程的相变应力，这也对焊接变形的减小有影响。

选取腹板中心轴上等距离 5 个点，测量焊接前后局部平面度。与非振动焊接工件的对比测量结果如表 3，图 5 所示。

表 3 腹板局部平面度变化

Table 3 Variation of local flatness in web plate

测点序号	振动焊接 d_{L_1} /mm	非振动焊接 d_{L_0} /mm
1	12	3
2	9	12
3	8	22
4	18	21
5	16	22

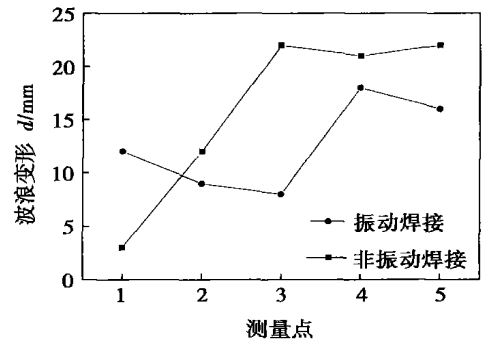

图 5 振动焊接与非振动焊接的变形比较

Fig. 5 Comparison of transformation in VWC and normal welding

从焊后变形对比曲线（图 5）可以看出，采用振动焊接后结构的总体变形明显减小。根据变形优化率 B 公式

$$B = \frac{d_{L_0} - d_{L_1}}{d_{L_0}} \times 100\%,$$

式中：d_{L_1} 为振动焊接条件下腹板局部平面度变化量；d_{L_0} 为非振动焊接条件下腹板局部平面度变化量。计算结果为总平均优化率达 21.3%。

3 结 论

（1）对高炉钢 BB503 电渣焊的试验表明，振动电渣焊工艺可以有效细化焊缝和热影响区粗晶区的晶粒，常规电渣焊接头侧弯合格率只有 25%，而振动电渣焊接头侧弯合格率达到 100%；且 6 m/s^2 的振动加速度比 3 m/s^2 的振动加速度在提高振动电渣焊接头综合性能上显示出明显优势。

（2）对 Q235B 材料 H 型钢的振动埋弧焊试验表明，振动埋弧焊工艺减小了焊后型钢的波浪变形，腹板的波浪变形控制在常规埋弧焊工艺的一半左右，型钢的焊接质量得到提高。 [下转第 98 页]

当发生应变时，长条状的M－A组元与基体之间的界面上容易产生微空洞和微裂纹，成为局部脆性区，并且长条状的M－A组元本身又不具有较大的塑性变形能力，会在裂纹长大的后期断开，造成解理断裂而降低韧性[6]，因此 $t_{8/5}$ 为 8 s 和 20 s 时冲击吸收功偏低；当 $t_{8/5}$ 为 40 s 时 M－A 组元的条片逐渐变短，分布均匀，大多失去了方向性，这样的显微组织具有相对较高的韧性；当 $t_{8/5}$ 继续增大时，韧性显著下降，其原因是M－A组元尺寸增大使M－A组元与铁素体基体的界面减少，导致裂纹的容易传播，M－A组元总量和尺寸的增大(体积分数大于4%，平均尺寸约为2.5 μm)，塑性的α相在变形时的滑移自由程减少，导致韧性降低。综上所述，当M－A组元的尺寸在1 μm，$t_{8/5}$＝40 s时微钙钢冲击韧度较好。

表2 M－A组元体积分数和平均尺寸

Table 2 Volume fraction and mean size of M－A constituents

冷却时间 $t_{8/5}$/s	M－A组元的体积分数(%)	M－A组元的平均尺寸 d/μm
8	0.46	＜1
20	2.1	＜1
40	2.91	1
80	4.27	2.5

3 结 论

(1) 经过中等冷却速度的焊接热循环后，微钙钢焊接粗晶热影响区中存在一定数量的粒状贝氏体。

(2) 用 Lepera 试剂腐蚀法制备的微钙钢试样，能够在光学显微镜下清晰看到粒状贝氏体中的M－A组元。

(3) 冷却速度对粒状贝氏体中M－A组元的形态和分布有显著的影响。$t_{8/5}$＝8 s时，M－A组元尺寸较小，且主要以长条状存在，并具有显著的方向性；$t_{8/5}$＝20 s和 $t_{8/5}$＝40 s时，M－A组元数量增加，尺寸变大，其形状除长条状以外，还有一定量的颗粒状，大多失去方向性；$t_{8/5}$＝80 s时M－A组元的数量减少，所占体积分数增加，尺寸较大，形状以颗粒状为主，均匀分布。

(4) 随着 $t_{8/5}$ 的增加，CGHAZ 冲击吸收功先增加然后下降。$t_{8/5}$＝40 s时，在各个温度下的吸收功均达到最高。

参考文献：

[1] Akihiko Kojima, Akihito Kiyose, Ryuji Uemori. Super high HAZ toughness technology with fine microstructure imparted by fine particles[J]. Nippon Steel Technical Report, 2004, 90(6): 3－5.

[2] Massaki, Nagahara, Hidenori, Fukami530 N/mm^2 tensile strength grade steel plate for multi-purpose gas carrier[J]. Nippon Steel Technical Report, 2004, 90(6): 11－13.

[3] 田德蔚，钱百年，斯重遥. 适用图像仪测定M－A相的腐蚀方法[J]. 物理测试，1994(2)：35－39.

[4] 田德蔚，钱百年，斯重遥. 用图像仪测定M－A组元的腐蚀方法的比较研究[J]. 理化检验－物理分册，1994，30(1)：28－30.

[5] 尹桂全，查显著，陆佰忠. STE355钢焊后显微组织中粒贝及其对韧性的影响[J]. 焊接学报，2003，24(2)：55－60.

[6] 赵 琳，张旭东，陈武柱. 800 MPa级低合金钢焊接热影响区韧性的研究[J]. 金属学报，2005，41(4)：392－396.

作者简介：贾坤宁，女，1978年出生，博士研究生。主要从事材料加工工程方面的研究工作，发表论文1篇。

Email：jiakunning@163.com

[上接第94页]

参考文献：

[1] 邹跃岐，赵玉成，徐建飞，等. 大型环形结构件焊接变形的分析及控制方法[J]. 焊接，2003(8)：40－41.

[2] 许德强，杨宏伟. 减少大型结构件焊接变形的工艺对策[J]. 工程机械，2003(02)：40－42.

[3] 朱政强，陈立功，倪纯珍. 振动焊接工艺的研究现状及发展方向[J]. 焊接，2003(5)：5－7.

[4] Goncharevich I F, Frolov K V, Rivin E I. Theory of vibratory technology[M]. New York: Hemisphere Publishing Corporation, 1990.

[5] 陈金涛，宫照坤，曲 牡，等. 振动焊接对焊缝力学性能影响[J]. 大连理工大学学报，2001，41(1)：35－37.

[6] 张国福，宋天民，尹成江，等. 机械振动焊接对焊缝及热影响区金相组织的影响[J]. 焊接学报，2001，22(3)：85－87.

[7] 管建军，宋天民，张国福，等. 机械振动对焊接熔池金属凝固过程的影响[J]. 抚顺石油学院学报，2001，21(4)：51－54.

[8] 谢春林，樊节斌，朱国巍. 振动焊接技术研究与应用[J]. 压力容器，2003，20(8)：8－13.

[9] 田锡唐. 焊接结构[M]. 北京：机械工业出版社，1982.

[10] 张丙尧. H型钢的焊接[J]. 河南化工，2002(3)：39－40.

作者简介：卢庆华，女，1978年出生，博士研究生。主要从事焊接结构强度及断裂方面的研究工作，发表论文4篇。

Email：aurora－luqh@sjtu.edu.cn

Abstract: The electrical signals of CO_2 arc welding contain plenty of welding information. The joint time-frequency analysis was used to study the electrical signals of CO_2 arc welding. The effect of analysis window selecting of short-time Fourier transform to the result of time-frequency analysis spectrum was discussed, and the conclusion that Hanning window has better time-frequency centralizing in analysis was gotten. Based on several welding currents and arc voltages in experiment, the characteristic of energy distribution and metal transfer was investigated by time-frequency analysis to get the information of short-circuiting transfer in electrical signals of CO_2 arc welding. The result of analysis in experiment shows that more information in electrical signals can be gotten by time-frequency analysis in CO_2 arc welding. This way has a good foreground in research and application.

Key words: joint time-frequency analysis; CO_2 arc welding; short-time Fourier transform

Effect of thermit composition on manual SHS welding for low carbon steel LI Zhizun, XIN Wentong, WU Bin, LI Baofeng (Advanced Material Institute, Ordnance Engineering College, Shijiazhuang 050003, China). p79—81

Abstract: Base on self-propagating high-temperature synthesis(SHS), a new method of welding called manual SHS welding is introduced. Since it is easy to carry and operate, this technique can be used in emergency maintenance. The effect of the thermit composition of the combustion welding rod on the welding of low carbon steel and the microstructure of weld were studied. The thermit was composed of (CuO+Al) and (Fe_2O_3+Al). It is shown that when the content of (CuO+Al) is higher than 50%, welding can successfully proceed. And combustion velocity becomes higher with the increasing of (CuO+Al) content. This is due to the higher combustion temperature and larger combustion heat of (CuO+Al) thermit. The tensile strength of weld becomes higher with the increasing of (Fe_2O_3+Al) content. This is due to the precipitation of the second phase rich in Fe, which can thin the Cu grain and strengthen the alloy. The combustion welding rod with 50% and 60% (CuO+Al) thermit is easy to operate and the tensile strength of weld are higher than 420 MPa.

Key words: manual self-propagating high-temperature synthesis welding; thermit; combustion velocity; tensile strength

Microstructure and residual stress of TA12 titanium alloy with electron beam welding FU Pengfei[1], HUANG Rui[2], LIU Fangjun[1], ZUO Congjin[1](1. Key Laboratory of High Energy Density Beam Processing Technology, Beijing Aeronautical Manufacturing Technology Research Institute, Beijing 100024, China; 2. Qian Han Pipe Factory, Chengdu Aircraft Industrial Group Co., Ltd., Chengdu, 610092, China). p82—84

Abstract: Weld configuration of TA12 titanium alloy is very good for electron beam welding(EBW). The main microstructure of weld is martensite, and the tiny rare earth rich phases is dispersedly distributed in the weld zone, and dimension whose configuration changes disciplinary along the joint. By hole drilling method measuring weld residual stresses, the results show that longitudinal stresses are higher than transverse stress, which present gradient distribution along the vertical direction of the weld. In the weld all the longitudinal residual stresses are tensile stresses, and whose peak stresses are lower than yield stresses, while the transverse stresses are very low pressure stresses. Along the weld direction in the central of the plate the residual stresses distributing are approximate equal.

Key words: TA12 titanium alloy; electron beam welding; rare earth phase; residual stress

Effects of shielding gas in CO_2 laser—MAG hybrid welding GAO Ming, ZENG Xiaoyan, HU Qianwu, YAN Jun (School of Optoelectronics Science and Engineering, Huazhong University of Science and Technology, Wuhan 430074, China). p85—88

Abstract: Shielding gas is acrucial factor for the process stability, weld penetration and joint quality of CO_2 laser—MAG (mental active gas) hybrid welding. However, the concerned researches about this field are very few. A serial trial investigating the effect of He—Ar and CO_2—Ar shielding gas on CO_2 laser—MAG hybrid welding was carried out on mild steel. The results show that different mixed shielding gases have different effects. The penetration depth and microhardness of He—Ar welds are hisher than that of CO_2—Ar welds. Because atomic oxygen is decomposed from CO_2 under high temperature and enters into welding pool, the surface tension coefficient changes and the direction of weld pool flow is changed. Consequently, CO_2—Ar weld reinforcement becomes flatter at $CO_2 \geqslant 30\%$ and the transition from arc zone to laser zone is flatter. Moreover, when $CO_2 > 30\%$, the process stability and microhardness of weld dramatically decrease.

Key words: laser welding; arc welding; hybrid welding; shielding gas; welding penetration

A CO_2 arc welding seam detection algorithm based on transition region YANG Fugang, SUN Tongjing, ZHANG Guangxian, PANG Qingle (School of Control Science and Engineering, Shandong University, Jinan 250061, China). p89—91

Abstract: In order to detect CO_2 arc welding seam, a new image segmentation method based on transition region is presented. Transition region is a special region located between the object and background in the real image, whose histogram has a wide and evenly hollow between two peaks. First, transition region of original image is determined by calculating the average grads of nonzero pixels of the image obtained through top-cut and bottom-cut transform, and then threshold can be obtained easily from transition region. It overcomes the effect of disturbance. Examinations indicate that it is a good method to detect CO_2 arc welding seam.

Key words: CO_2 arc welding; edge detection; seam detection; transition region

Application of vibratory welding technology to large-scale welding components LU Qinghua, CHEN Ligong, NI Chunzhen, RAO Delin (School of Materials Science and Engineering, Shanghai Jiaotong University, Shanghai 200030, China). p92—94, 98

Abstrat: The vibratory conditioning process was investigated

in the electroslag welding of blast furnace steel. The metallographs show that a grain refined joint is produced. The residual stress and side bend property were carried out in different vibratory conditions (0, 3 and 6 m/s^2). Welding deformations is a very serous problem in welding of H-section steel. The welding deformation of the H-sesults of the test have fully proved that vibratory conditioning technology can effectively reduce residual stress, and improve the comprehensive properties of welded joints, and reduce the residual welding deformation, which guarantee the production quality.

Key words: vibratory welding; side bend; H-section steel; welding deformation

Effect of granular bainite in microstructure after welding on impact toughness for micro-calcium steel JIA Kunning, ZHAO Hongyun, GAO Cairu, WANG Guodong (State Key Laboratory of Rolling and Automation, Northeastern University, Shenyang 110004, China). p95—98

Abstract: The effects of technology parameters of simulated welding thermal cycle(cooling time $t_{8/5}$) on microstructures and impact toughness of CGHAZ in micro-colcium steel were studied. The M—A constituents in granular bainite were etched by Lepera reagent. The pattern, quantity and distribution of M—A constituents with different $t_{8/5}$ were studied in optical microscope and TEM. The research shows that when the cooling rate is lower the M—A constituents are bacillary and directional, when the cooling rate is higher the M—A constituents are granular and direction-free. When $t_{8/5}$ = 40 s the impact toughness is better than other cooling time.

Key words: simulated welding thermal cycle; granular bainite; M—A constituents; toughness

Effects of gas trapped in nickel alloy coating on corrosion behavior of coating deposited by HVOF ZHAO Weimin[1, 2], WANG Yong[1] (1. School of Mechanical and Electrical Engineering, China University of Petroleum, Dongying 257061, Shandong, China; 2. School of Material Science and Engineering, Xi'an Jiaotong University, Xi'an 710049, China). p99—102, 107

Abstract: The NiCrBSi alloy powders were sprayed to a steel substrate using high velocity oxy-fuel(HVOF) after which some coatings were heat treated at 600 ℃ in vacuum for 2 hours, and corrosion behavior of the as-sprayed coating and heat-treated coating in 3.5% NaCl aqueous solution was investigated using electrochemical impedance spectroscopy. The results show that effects of gas trapped in nickel alloy coating on corrosion potential and corrosion resistance of the coating are great. The corrosion potential of as-sprayed coating is higher than that of the gas-removed coating which has been heat-treated in vacuum, because the gas can decrease the electric charge density in electrochemical double layer thus heighten the corrosion potential. The coating can be densified by heat-treatment, but the corrosion resistance of as-sprayed coating is higher than that of the heat-treated coating, so the effects of gas on corrosion resistance are greater than that of microstructure. However, the influence of gas is short-term and the corrosion potential and corrosion resistance decrease dramatically at the early stage of corrosion. The corrosion behavior of coating is determined by microstructure finally.

Key words: high velocity oxy-fuel spraying; metallic coating; corrosion; gas; heat treatment

Electrochemical corrosion properties for weld metal of austenitic stainless steel ZHANG Junwang[1], WANG Wenxian[1], HUANG Yanping[2], WANG Baodong[2], LIU Xu[1] (1. School of Material Science and Engineering, Taiyuan University of Technology, Taiyuan 030024, China; 2. Shanxi Zhongtong High-tech Co., Ltd, Taigu 030800, Shanxi, China). p103—107

Abstract: The electrochemical corrosion property of weld metal of the austenitic stainless steel SUS316 in TIG welding, MIG welding and TIG welding with welding wire (TIG+M) were tested with PASTAT30 type potentiostat. The results show that corrosion resistance of weld metal in TIG welding is the least compared with base metal and welded metal in MIG welding and TIG welding with H0Cr19Ni12Mo3 welding wire not only in 5% HCl but also in 9.8% H_2SO_4. And the order of electrochemical corrosion resistance in 9.8% H_2SO_4 is base metal, welded metal in TIG+M, MIG welding and TIG welding. The order in 5% HCl is base metal, welded metal in MIG welding, TIG+M and TIG welding. Passivation zone in H_2SO_4 is more length than which in HCl, so corrosion resistance of the austenitic stainless steel in H_2SO_4 is better than which in HCl. Huey test was also carried out, and the result of this test was coincident with the result of the electuochemical corrosion test in 9.8% H_2SO_4.

Key words: austenitic stainless steel SUS316; tungsten inert-gas welding; weld metal; electrochemical corrosion resistance

Preparation methods of particle reinforced surface metal matrix composites ZHAO Minhai, GUO Mianhuan, FENG Jicai, LIU Aiguo (State Key Laboratory of Advanced Welding Production Technology, Harbin Institute of Technology, Harbin 150001, China). p108—112

Abstract: Preparation methods of particle reinforced surface metal matrix composites were classified according to the thermal sources used and the feeding of reinforcing ceramic particles. Hardfacing, laser cladding, laser melt injection and plasma melt injection were introduced, and the virtues and defects of all the methods were discussed. Metallurgical bonding between the substrate and the coating could be achieved with hardfacing, and it was very effective. Energy input could be controlled precisely in laser cladding process, and the cooling rate was high, so the thermal distortion was very little. While, cracks always appeared in the hardfacing and laser cladding process. Laser melt injection was not restricted by the weldability of the substrate, and coatings with uniformly distributed strengthening phases could be achieved with it, so cracks could be avoided in the laser melt injection process. The plasma melt injection process was similar to the laser melt injection process, and gradient composites with strengthening phases varying from 0 to 100% could be achieved with it. Cracks caused by unevenly distributed strengthening phases could be avoided. The investment for the plasma melt injection process was very low, and it was cost effective.

Key words: particle reinforced; surface metal matrix composites; preparation methods